Plant Physiology and Biochemistry 140 (2019) 96–104

Contents lists available at ScienceDirect

Plant Physiology and Biochemistry

journal homepage: www.elsevier.com/locate/plaphy

Research article

Strand-specific RNA-seq based identification and functional prediction of lncRNAs in response to melatonin and simulated drought stresses in cassava

Zehong Ding[a,*,1], Chunlai Wu[a,b,1], Weiwei Tie[a], Yan Yan[a], Guangyuan He[b,***], Wei Hu[a,**]

[a] Key Laboratory of Biology and Genetic Resources of Tropical Crops, Institute of Tropical Bioscience and Biotechnology, Chinese Academy of Tropical Agricultural Sciences, Xueyuan Road 4, Haikou, Hainan, China

[b] Genetic Engineering International Cooperation Base of Chinese Ministry of Science and Technology, Chinese National Center of Plant Gene Research (Wuhan) HUST Part, Key Laboratory of Molecular Biophysics of Chinese Ministry of Education, College of Life Science and Technology, Huazhong University of Science and Technology (HUST), Wuhan, China

ARTICLE INFO

Keywords:
Cassava (*Manihot esculenta* Crantz)
Long noncoding RNAs
Strand-specific RNA-Seq
Polyethylene glycol (PEG) treatment
Melatonin treatment

ABSTRACT

Melatonin (MT) plays important roles in mediating plant responses to abiotic stresses such as drought. lncRNAs also play crucial roles in regulating responses to drought stress, however, their roles in MT-mediated drought stress responses in plants remain largely unknown. In this study, a total of 1405 high-confidence lncRNAs were identified in leaves of cassava, an important food crop in tropical and sub-tropical regions, using strand-specific RNA-seq technology. Of which, 185 were differentially expressed between polyethylene glycol (PEG) or MT treatment and the control condition. Trans-regulatory co-expression network revealed that MT-uniquely-responsive lncRNAs were mainly involved in tetrapyrrole synthesis, cytochrome P450, and cell wall modification; PEG-uniquely-responsive lncRNAs mainly participated in RNA regulation of transcription, calcium signaling, mitochondrial electron transport/ATP synthesis, hormone metabolism, and transport; and MT and PEG both-responsive lncRNAs were mainly involved in light reaction, light signaling, FA synthesis and FA elongation, secondary metabolism, and tetrapyrrole synthesis. In addition, 28 lncRNA-mRNA pairs referred to *cis*-acting regulation were identified, and these lncRNAs regulated the expression of their neighboring genes mainly through calcium signaling, RNA regulation of transcription, ABA and ethylene metabolism, and redox homeostasis. Besides, 78 lncRNAs (especially TCONS_00003360, TCONS_00015102, and TCONS_00149293) responsive to MT and/or PEG treatment were identified as putative targets of cassava known miRNAs. These findings provide a comprehensive view of the lncRNAs and their roles in response to MT and drought stress in cassava, which will enable in-depth functional analyses in the near future.

1. Introduction

Cassava (*Manihot esculenta* Crantz) is an important cash crop for farmers in tropical and sub-tropical areas, and it provides staple food for over 750 million people around the world (Utsumi et al., 2012). Because of its starch-enriched root, cassava is considered as one of the major sources for starch production, bio-fuel, and animal feed. Cassava is generally tolerant to drought, however, severe drought stress greatly depresses its growth and development, and finally reduces its economic yield (Okogbenin et al., 2013). Thus, it is of great importance to increase our understanding of the molecular mechanisms of drought stress in cassava.

Many studies have demonstrated that melatonin (MT) increases drought tolerance and plays multiple roles in plants including regulating water balance, delaying leaf senescence, promoting lateral root formation, protecting photosynthetic systems, and modulating nitro-oxidative homeostasis and proline metabolism (Antoniou et al., 2017; Arnao and Hernandez-Ruiz, 2018; Wang et al., 2013b; Zhang et al., 2013). Specifically, drought stress increases the accumulation of reactive oxygen species (ROS) and causes a rapid and massive induction of MT, which in turn increases the antioxidant capacity and ROS homeostasis in drought-stressed plants (Cui et al., 2017; Shi et al.,

* Corresponding author.
** Corresponding author.
*** Corresponding author.
E-mail addresses: dingzehong@itbb.org.cn (Z. Ding), wuchunlai19900109@126.com (C. Wu), tieweiwei@itbb.org.cn (W. Tie), yoyoyan7758@163.com (Y. Yan), hegy@hust.edu.cn (G. He), huwei2010916@126.com (W. Hu).
[1] These authors contributed equally to this work.

https://doi.org/10.1016/j.plaphy.2019.05.008
Received 31 January 2019; Received in revised form 5 May 2019; Accepted 6 May 2019
Available online 10 May 2019
0981-9428/

2016). As one of the most important ROS, H_2O_2 directly participates in the regulation of abscisic acid (ABA)-mediated stomatal movement, which represents an essential physiological response of plants to drought stress. Importantly, the accumulation of ABA levels is associated with the formation of ROS in plant cells, since H_2O_2 is accordingly reduced when less endogenous ABA is available (Ye et al., 2011). Recent studies revealed that MT pre-treatment significantly down-regulates *MdNCED3* (a key gene involved in ABA biosynthesis) to reduce ABA content and enhances the activities of antioxidant enzymes to detoxify H_2O_2, supporting that both ABA and H_2O_2 signaling pathways play a central role in MT enhanced drought tolerance (Li et al., 2015). On the other hand, exogenous MT treatment also can increase the concentration of ABA which is required for MT-induced stimulation of antioxidant defense under cold stress (Fu et al., 2017). With the rapid development of high-throughput sequencing technology, many studies have documented that MT alters the expression of many genes related to calcium-dependent signaling, transcription factors (such as the members of WRKY and NAC), and redox homeostasis (Weeda et al., 2014; Zhang et al., 2015). Interestingly, the expression levels of these genes were also significantly altered under drought condition (Fu et al., 2016; Zeng et al., 2017), indicating that these genes might play a major role in gene expression regulation of MT-mediated drought stress, which needs to be further elucidated.

Long noncoding RNAs (lncRNAs) are RNA transcripts with more than 200 bp in length but lacking coding capacity. Based on the position of lncRNAs and protein-coding genes, lncRNA are classified into types of long intergenic noncoding RNAs (lincRNAs), long noncoding natural antisense transcripts (lncNATs), and long intronic noncoding RNAs (Chekanova, 2015). Previously lncRNAs were considered as transcriptional noises because of their low expression levels, but now emerging evidences have demonstrated that lncRNAs play important roles in regulating responses to abiotic stresses such as drought. Functional analyses further revealed that lncRNAs were involved in the transcriptional and post-transcriptional regulation of gene expression either in *cis* or in *trans* by sequence complementarity or homology with RNAs or DNAs, and/or by structure, forming molecular frames and scaffolds for the assembly of macromolecular complexes (Chekanova, 2015). Besides, lncRNAs can be directly targeted by miRNAs for cleavage (Fan et al., 2015; Shuai et al., 2014). More interestingly, lncRNAs can also function as miRNA target mimics to interact with miRNAs which usually regulate the expression of their mRNA targets through cleavage in plants (Franco-Zorrilla et al., 2007; Wu et al., 2013). To date, hundreds of drought-responsive lncRNAs have been identified in plants including *Arabidopsis* (Di et al., 2014), rice (Yuan et al., 2018), maize (Zhang et al., 2014), Populus (Shuai et al., 2014), cotton (Lu et al., 2016), and cassava (Li et al., 2017). In addition, accumulating evidences showed that MT participated in the regulation of lncRNAs with the involvement of miRNAs for certain functions (Cai et al., 2016; Zhang et al., 2018). However, lncRNAs and their roles in MT-mediated drought stress responses in plants remain largely unknown.

To gain new insights into the involvement of lncRNAs in MT-mediated drought stress in cassava, in this study, we applied a strand-specific RNA-seq (ssRNA-seq) sequencing approach to investigate the genome-wide transcriptome changes of cassava leaves under MT treatment and polyethylene glycol (PEG)-induced drought stress. Subsequently, the lncRNAs responsive to MT and PEG treatment were identified, their expression patterns were revealed, and the potential functions of these lncRNAs were predicted and analyzed. These findings will expand our knowledge of lncRNAs in MT-mediated drought stress in cassava.

2. Materials and methods

2.1. Plant materials and experimental treatments

The stems of cassava variety 'Arg 7′ were cut into ~15 cm in length with two to three buds and cultured in pots (height × bottom diameter × upper diameter = 18.8 cm × 14.8 cm × 18.5 cm) with soil and vermiculite (1:1) in the glass house at the Chinese Academy of Tropical Agricultural Sciences, Haikou, China. The growth conditions were 16 h/35 °C in the day and 8 h/20 °C in the night with a relative humidity of 70%. Ninety days later, uniform cassava seedlings were selected and irrigated with 20% PEG 6000 solution for drought and 100 μM MT solution for MT treatment, respectively, for a total of 11 days with a frequency of once every four days. The seedlings irrigated with tap water were used as control. The first fully expanded leaves were collected from three individual plants at 0, 0.5, 1, 3, 5, 7, 9, and 11 d, respectively, to measure peroxidase (POD) activity, H_2O_2, MT, and ABA content. Those samples collected at 0, 5, 7, and 9 d were also selected for ssRNA-seq sequencing.

2.2. Physiological measurement

The H_2O_2, MT, and ABA content, and POD activity were measured spectrophotometrically. As previously described (Hu et al., 2016), about 0.5 g leaves were ground and homogenized in 5 mL extraction buffer containing 0.05 M phosphate buffer (pH7.8), then the homogenate was centrifuged at 10000 g for 10 min at 4 °C, and the supernatant was collected for further analysis. The MT and ABA contents were determined using the plant enzyme-linked immunosorbent assay (ELISA) kits (ml036336 and ml077235, MeiLian Biotechnology, Shanghai, China). The H_2O_2 content and POD activity were determined using the corresponding assay kits (A064 and A084, Nanjing Jiancheng, Nanjing city, China), according to the manufacturer's instructions.

2.3. Library construction and high-throughput sequencing

The total RNA extraction, whole transcriptome libraries preparation, and RNA sequencing were performed by the MajorBio Bio-pharm Technology Co., Ltd. (Shanghai, China). The RNA-seq libraries were constructed using Illumina TruSeq™ RNA sample prep Kit (Illumina, San Diego, CA, USA) with Ribo-Zero Magnetic kit for rRNA depletion according to the manufacturer's instructions, and subsequently sequenced on a HiSeq 4000 instrument to generate paired-end reads of 150 nucleotides in length.

2.4. Bioinformatics identification of lncRNAs

After removing the adaptor sequences and filtering out low-quality reads, clean reads were obtained and subsequently mapped to the cassava reference genome using Tophat 2.0 (Trapnell et al., 2009) with '-library-type fr-firststrand' parameters. Cufflinks pipeline (Trapnell et al., 2012) was applied to assemble reads into transcripts, and the assembled transcripts found in at least two samples were selected for further analysis. The expression levels were calculated as fragments per kilobase per million mapped reads (FPKM). For identification of lncRNA, a few vigorous steps were performed. Firstly, the transcripts that with length < 200 bp, that with exon number < 2, that with ORF length > 300, that with minimal reads coverage < 3, and that overlapped with known protein-coding genes on the same strand were removed. Secondly, the transcripts with coding potential were removed based on the evaluation of CPC (Kong et al., 2007), CPAT (Wang et al., 2013a), and CNCI (Sun et al., 2013). Thirdly, the transcripts with known protein domains were also excluded according to Pfam-HMM (Eddy, 2009). The remaining transcripts were considered as reliable lncRNAs. Differentially expressed (DE) lncRNAs between PEG or MT treatment and the control condition (CK, 0 d) were identified, respectively, setting FDR < 0.05 and $|\log_2 FC| > 1$.

2.5. LncRNA target prediction and functional enrichment

To identify the target genes in trans-regulation, DE lncRNAs,

together with their co-expressed DE genes, were analyzed by the standard procedure of WGCNA (Langfelder and Horvath, 2008). Briefly, the Pearson correlation matrix of the expression profile was calculated and then transformed into an adjacency matrix, which was subsequently applied to construct the gene co-expression network. A soft thresholding power (β = 16) was selected to render the network scale-free. Genes and lncRNAs were assigned into different modules based on the dynamic tree cut method by setting minClusterSize = 30. The lncRNAs and genes within the same group (module) were of similar expression patterns and potentially in trans-regulation. For the functional prediction of lncRNAs in trans-regulation, cassava loci were functionally annotated and classified into hierarchical categories based on MapMan (Thimm et al., 2004), and the significantly over-represented functional categories were determined according to the Fisher's exact test as previously reported (Fu et al., 2016).

To identify the target genes in cis-regulation, DE lncRNAs and the adjacent protein-coding genes, which were spaced 10 k/100 k up- and down-stream of these lncRNAs (Lu et al., 2016), were selected and also subjected to co-expression analysis. The lncRNA-mRNA pairs that were co-expressed and closely located were in cis-acting regulatory relationships.

2.6. Prediction of lncRNAs acting as miRNA targets

The miRNAs, targeting the lncRNAs, were predicted by submitting all of the discovered DE lncRNAs and the cassava miRNAs (miRBase Release 22, March 2018) to psRNATarget (Dai et al., 2018), with less than three mismatches and G/U pairs allowed within the lncRNA-miRNA pairing regions. The interaction networks of miRNAs and the targeted lncRNAs were visualized using Cytoscape (Shannon et al., 2003).

2.7. qRT-PCR analysis

For the validation of ssRNA-seq results, eight lncRNAs differentially expressed under PEG and/or MT conditions were selected and confirmed by qRT-PCR with primers listed in Table. S1. The qRT-PCR reaction was conducted with SYBR Premix Ex Taq (Takara, Dalian, China) in 20 μL mixture containing ~100 ng of cDNA template, 0.5 μL of each primer (10 μmol), 0.4 μL of ROX reference dye II (50 ×), and 10 μL of SYBR Premix Ex Taq (2 ×). The qRT-PCR was performed on a Stratagene Mx3000P instrument (Stratagene, CA, USA), and the conditions were as follows: 30 s at 95 °C; followed by 40 cycles of 10 s at 95 °C and 30 s at 60 °C. Then, a thermal denaturing step generating the melt curves was followed to verify the amplification specificity. β-actin gene was used as the endogenous control (Fu et al., 2016). Each sample was measured in triplicate, and the relative expression levels were calculated using the $2^{-\Delta\Delta Ct}$ method.

3. Results

3.1. Physiological variations in response to PEG and MT treatments

To investigate the dynamic changes of cassava in response to PEG and MT treatments, several physiological traits, including H_2O_2, MT content, ABA content, and POD activity that are important parameters reflecting the physiological status of plant cells under abiotic stress, were measured under PEG and MT treatments across eight time points (0, 0.5, 1, 3, 5, 7, 9, and 11 d) in leaves. Overall, these physiological traits were not significantly changed during the whole treatment under control condition (Fig. 1).

Under PEG treatment, the H_2O_2 content was greatly increased from 0 to 1 d, then declined at 3 d and increased at 5 and 7 d, and finally declined at 9 and 11 d (Fig. 1A). Under MT treatment, the H_2O_2 content was gradually increased from 0 to 7 d, then declined at 9 and 11 d (Fig. 1A), which might reflect the demand of MT to reduce damages caused by oxidative stress.

Overall, the changes of MT content were consistent with that of H_2O_2 content. Under PEG treatment, the MT content was increased from 0 to 3 d, then decreased at 5 and 7 d, and finally increased at 9 and 11 d, exhibiting an opposite trend of H_2O_2 content (Fig. 1B). These results also indicated that MT can effectively eliminate oxidative damages under abiotic stress. Similar changes of MT content were observed between MT and PEG treatment, although the former showed much higher MT levels than the latter.

Interestingly, very similar trends of ABA content were observed between PEG and MT treatment: the ABA content was slightly increased from 0 to 3 d, then sharply increased at 5 and 7 d, and finally declined at 9 and 11 d (Fig. 1C), suggesting that similar ABA-involved signaling pathways were triggered in cassava leaves when they were treated with PEG and MT treatment.

Under PEG treatment, POD activity was significantly increased from 0 to 3 d, and then slightly varied until 11 d. Similar change of POD activity was observed under MT treatment, although its activity was much lower from 0 to 3 d but maintained at a relatively constant level from 5 to 11 d compared with that of PEG treatment (Fig. 1D).

Subsequently, ssRNA-seq was employed to investigate the expression changes in cassava leaves at 0, 5, 7, and 9 d after PEG and MT treatments to further reveal the variations at the transcriptional level.

3.2. High-throughput sequencing

In total, 1107 million raw reads of 150-bp in length were obtained from 14 libraries (7 samples × 2 replicates) by paired-end sequencing on Illumina HiSeq 4000 platform. After trimming adapters and removing low quality reads, about 1095 million clean reads were kept, and ~62.6% of them were mapped to the cassava reference genome for further analysis. The total length of all the mapped reads was over 164 gigabases (Gb), representing about 280-fold coverage of the cassava genome. Subsequently, a ssRNA-seq computational pipeline (Fig. 2) was implemented for lncRNA identification.

3.3. Identification and characterization of lncRNA

In total, 166 477 transcripts were detected after transcriptome reconstruction of all ssRNA-seq data using cufflinks. Of which, 99 104 (~59.5%) transcripts were overlapped with 32751 protein-coding genes (representing ~99.1% genes of the cassava genome) based on the reference gene annotation. Subsequently, these transcripts were preliminarily filtered by five filtering steps (e.g., transcript length ≥ 200 bp, exon number ≥ 2, and so on, Fig. 2), then the remaining transcripts were further subjected to coding potential filtering using different softwares such as CPC and CNCI, and only the ones that have no protein-coding capacity were kept. Finally, 1405 lncRNA candidates, containing 1081 intergenic lncRNAs and 324 anti-sense lncRNAs, were identified according to their genomic locations.

Subsequently, we mapped these lncRNAs to the 18 chromosomes of the cassava genome, and found that more anti-sense lncRNAs were located on chromosome 12 and 13 than other chromosomes. Compared with anti-sense lncRNAs, intergenic lncRNAs were more evenly distributed across these chromosomes without a preference of location (Fig. 3A). We then assessed the length and exon number of lncRNA transcripts. The median lengths of these anti-sense and intergenic lncRNAs were 1058 and 1112 nucleotides (nt), respectively, and most of them were shorter than 3000 nt (Fig. 3B). Similarly, very close trends of the distribution of exon number were observed between anti-sense and intergenic lncRNAs: most (~50%) of the cassava anti-sense and intergenic lncRNAs contained two exons, while the number of lncRNAs steadily decreased as the exon number increased (Fig. 3C). We also estimated the expression levels of lncRNAs using fragments per kilobase of exons per million fragments mapped (FPKM) and found that anti-sense and intergenic lncRNAs were expressed at similar levels.

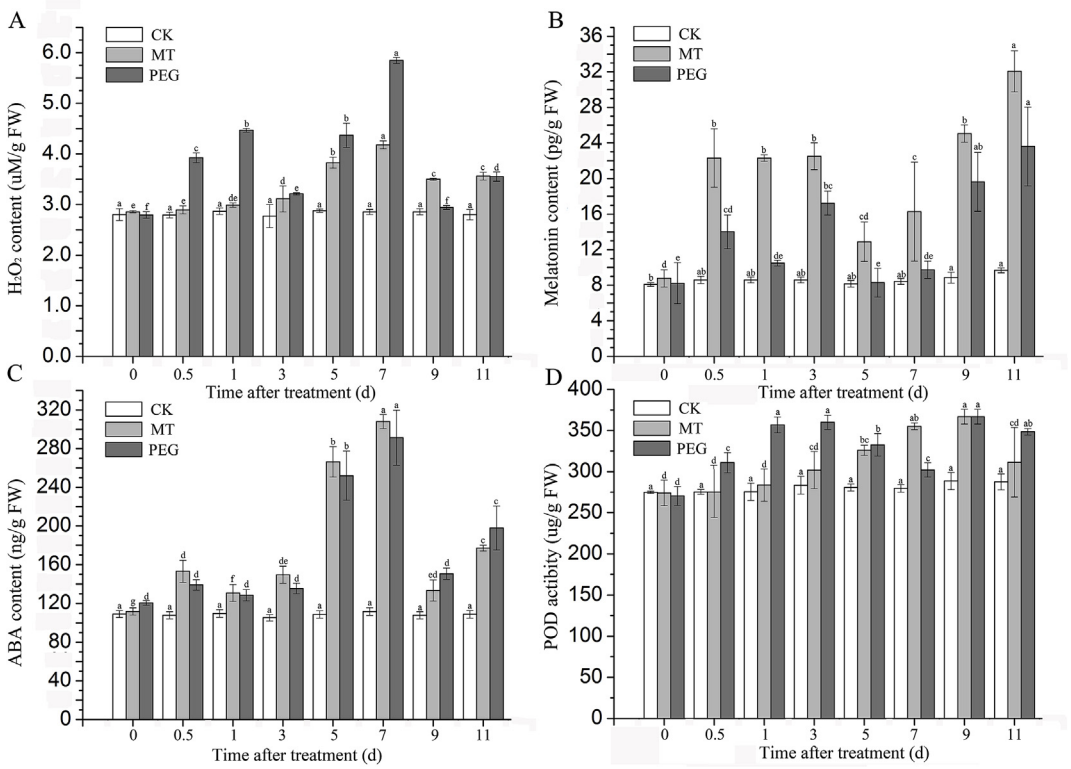

Fig. 1. Physiological investigation of H_2O_2, MT, and ABA content and POD activity in response to PEG and MT treatments. Values are means of three replicates ± SD. Different letters indicate means that are significantly different at $P < 0.05$ level among different time-points under the same treatment.

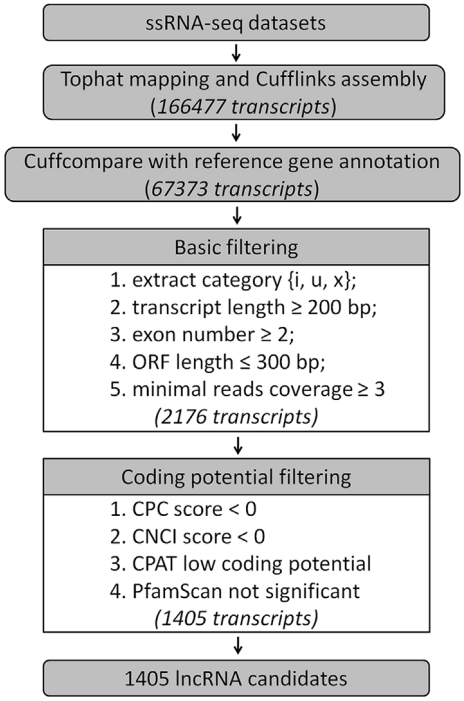

Fig. 2. Computational pipeline used for lncRNA identification.

Together, these results provide a general overview of the characterization of lncRNA in response to abiotic stresses in cassava.

3.4. Expression profiling and functional characterization of DE lncRNAs in trans-regulation

To reveal the transcriptional changes of lncRNAs affected by abiotic stresses, DE lncRNAs were identified by comparing their expression levels between the control and PEG or MT treatments, respectively. In total, 185 DE lncRNAs were identified. Of which, 75 (40%) were uniquely identified under PEG treatment, 68 (37%) were uniquely identified under MT treatment, and only 42 (23%) were commonly identified in response to both PEG and MT treatments (Fig. 3D).

To explore the potential functions of DE lncRNAs that were uniquely or commonly identified in PEG and MT treatments, these lncRNAs, together with 1218 DE genes in response to either PEG or MT stress, were selected and subjected to co-expression and functional enrichment analysis. Then, the enriched functions of DE genes could be used to predict the functions of lncRNAs that were co-expressed with these DE genes.

A total of seven groups (G1-G7) were mainly identified based on their expression patterns (Fig. 4A). There were 32 lncRNAs in group G1. These lncRNAs expressed highest in the control but their expression levels were greatly depressed in both MT and PEG treatments. MapMan enrichment showed that these lncRNAs were mainly involved in FA synthesis and FA elongation, nitrate metabolism, light reaction of photosynthesis, light signaling, secondary metabolism, and tetrapyrrole synthesis (Fig. 4B).

There were 20, 14, and 16 lncRNAs in groups G2 to G4, in which the expression levels of lncRNAs were exclusively induced under MT treatment with a preference of different time-points. The enriched categories included tetrapyrrole synthesis in G2, cytochrome P450 in G3, and cell wall modification in G4, respectively (Fig. 4B).

There were 20, 12, and 25 lncRNAs in groups G5 to G7. On the

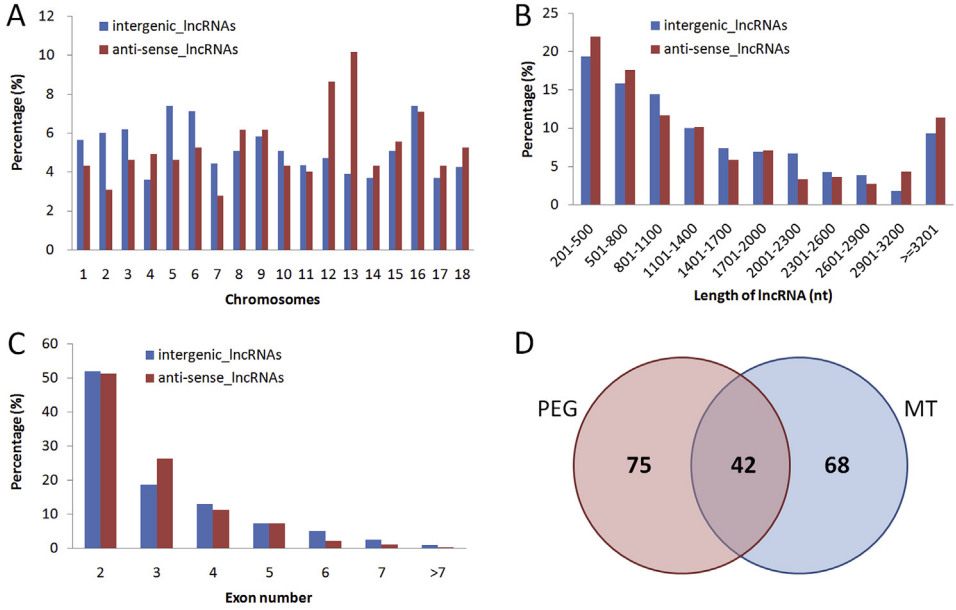

Fig. 3. Characterization of cassava lncRNAs in response to PEG and MT treatments. (A) Chromosome, (B) transcript length, and (C) exon number distributions of anti-sense and intergenic lncRNAs. (D) Distribution of DE lncRNAs between PEG and MT treatments.

contrary, the expression levels of these lncRNAs were exclusively induced under PEG treatment. Compared with G2 to G4, more significantly enriched categories were found in G5 to G7. The enriched categories in G5 included cellulose synthesis, ethylene metabolism, mitochondrial electron transport/ATP synthesis, RNA regulation of transcription, and calcium signaling, and those in G6 included jasmonate metabolism, minor CHO metabolism of raffinose family, abiotic stress, and transport. Several categories, including ABA metabolism, cytochrome P450, and secondary metabolism of isoprenoids, were significantly enriched in group G7 (Fig. 4B).

Taken together, these results indicated that MT-uniquely-responsive lncRNAs were mainly involved in tetrapyrrole synthesis, cytochrome P450, and cell wall modification; PEG-uniquely-responsive lncRNAs mainly participated in RNA regulation of transcription, calcium signaling, mitochondrial electron transport/ATP synthesis, hormone metabolism, and transport; and MT and PEG both-responsive lncRNAs were mainly involved in light reaction of photosynthesis, light signaling, FA synthesis and FA elongation, secondary metabolism, and tetrapyrrole synthesis.

3.5. Functional characterization of DE lncRNAs in cis-regulation

To further explore the possible functions of stress-responsive DE lncRNAs, protein-coding genes, which were spaced 10 k/100 k upstream and downstream of these lncRNAs, were selected and subjected to co-expression analysis. The lncRNA-mRNA pairs, which were co-expressed and closely located, were in *cis*-acting regulatory relationships and were specifically attractive.

A total of 28 lncRNA-mRNA pairs referred to *cis*-acting regulation were identified (Table. S2). Although most genes referred to these lncRNA-mRNA pairs were functionally unknown, there still were a few lncRNAs whose functions can be predicted by the well-annotated genes in *cis*-regulation relationship. For examples, TCONS_00046155 and TCONS_00129136 were responsive to both MT and PEG treatment, the former was spaced 2780 bp upstream of Manes.05G018500 encoding a SAUR-like auxin-responsive protein, while the latter was located 3270

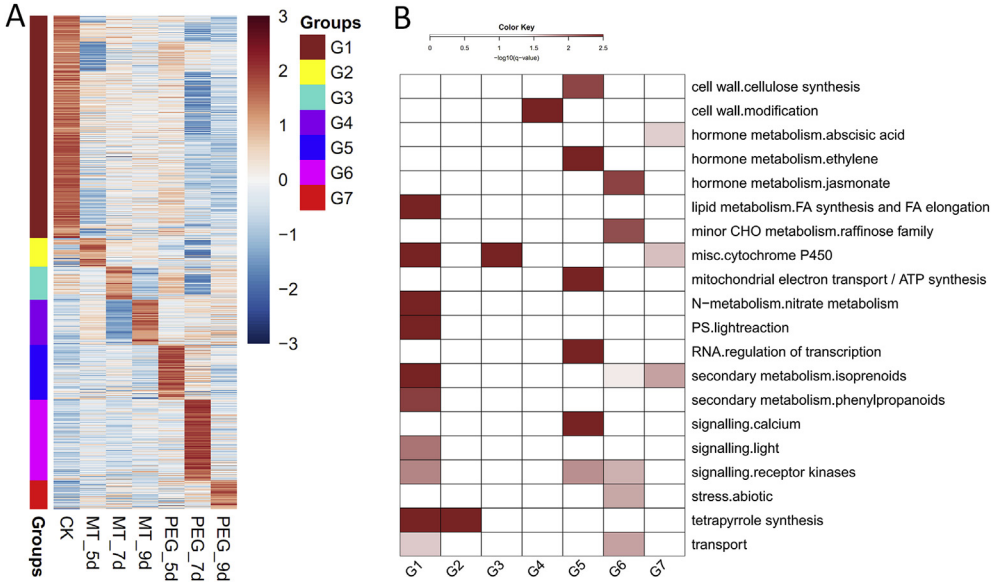

Fig. 4. Co-expression analysis of lncRNAs and mRNAs. (A) Heatmap of 185 DE lncRNAs and 1218 DE mRNAs, which were clustered into seven groups. Rows represent row-scaled expression values of genes/lncRNAs under the control (CK, 0 d), MT treated (prefixed with 'MT'), and PEG-treated (prefixed with 'PEG') conditions. (B) Functional category enrichment of each group presented in (A).

bp downstream of Manes.15G048700 coding a pectin lyase-like protein referred to cell wall degradation, suggesting possible related roles of these two lncRNAs. TCONS_00005423, TCONS_00035542, and TCONS_00005041 were exclusively responsive to MT treatment. Of which, TCONS_00005423 was located 6920 bp upstream of a NAC transcriptional factor (Manes.01G238300) and 8541 bp downstream of a calcium-binding protein (Manes.01G238000), TCONS_00035542 was spaced 6696 bp upstream of Manes.04G105000 involved in ethylene signal transduction, and TCONS_00005041 was located 3997 bp downstream of Manes.01G215100 participated in redox homeostasis. TCONS_00011480 and TCONS_00085215 were exclusively responsive to PEG treatment. Of which, TCONS_00011480 was located 6014 bp downstream of Manes.01G234200 coding a Ca^{2+} activated K^+ channel protein, whereas TCONS_00085215 was spaced 549 bp downstream of Manes.10G067700 involved in ABA metabolism (Table. S2).

Together, these results suggested that the DE lncRNAs, which might participate in abiotic stresses of PEG and MT treatments in *cis*-acting, regulated the expression of their neighboring genes through calcium signaling, RNA regulation of transcription, hormone metabolism (such as ABA and ethylene), and redox homeostasis.

3.6. Functional prediction of lncRNAs acting as miRNA targets

Since lncRNAs can be directly targeted by miRNAs for cleavage and degradation, the crosstalk between lncRNAs and miRNAs was investigated by exploring the lncRNAs acting as targets of cassava known miRNAs.

In total, 78 lncRNAs were predicted as targets of 149 miRNAs from 37 miRNA families. Of which, 21 lncRNAs were responsive to both MT and PEG treatment, and 27 and 30 lncRNAs were exclusively responsive to MT and PEG treatment, respectively. The details of miRNAs and their targeting lncRNAs were available in Table. S3, and their interactions were visualized by Cytoscape in Fig. 5. To date, many known drought-responsive and ABA-induced miRNAs (e.g., miR156, miR159, miR167, miR169, and miR172) were identified in plants (Ferdous et al., 2015). Interestingly, in this work, four of them (including mes-miR156, mes-miR169, mes-miR172, and mes-miR159) showed the most connections to lncRNAs, suggesting they might play similar roles in response to MT and PEG treatment in cassava, e.g., through a miRNA-lncRNA interaction regulation. TCONS_00003360, TCONS_00015102, and TCONS_00149293 were the top three lncRNAs with the most connections to miRNAs. Of which, TCONS_00003360 was responsive to both MT and PEG treatment, while TCONS_00015102 and TCONS_00149293 were exclusively responsive to MT and PEG treatment, respectively. Notably, TCONS_00015102 was targeted by mes-miR156 and mes-miR169, whereas TCONS_00149293 was targeted by mes-miR156, mes-miR159, mes-miR169, and mes-miR172, strongly suggested that these lncRNAs participated in ABA-involved gene regulation in abiotic stress of cassava via miRNA-lncRNA interaction, and their functions deserved to be further characterized.

3.7. Validation of lncRNAs expression by qRT-PCR

In total, eight interested lncRNAs, which were related to hormone metabolism, cell wall, calcium signaling, transport, and RNA regulation of transcription, were selected and analyzed by quantitative real-time PCR (qRT-PCR). As shown in Table. S1, the expression patterns of the stress-responsive lncRNAs were relatively consistent between RNA-seq and qRT-PCR (R = 0.74–0.97), suggesting that the lncRNA expression patterns based on RNA-seq data were reliable.

4. Discussion

LncRNA is a type of new molecule playing various important roles in a wide range of biological processes, including developmental regulation and abiotic stress responses. With the rapid development of high-throughput technology, RNA-seq has become a widely used and effective approach to identify lncRNAs in plants (Li et al., 2014; Lu et al., 2016). In this study, a total of 1405 lncRNAs, including 1081 intergenic lncRNAs and 324 anti-sense lncRNAs were identified in response to PEG and MT treatments in cassava using strand-specific RNA-seq strategy. The number of lncRNAs was far less than that identified in rice and *Arabidopsis* (Di et al., 2014; Yuan et al., 2018), but about two-fold of that identified previously in cassava (Li et al., 2017), indicating that the number of lncRNAs identified by sequencing might depend largely on the species, sequencing depth, and the criteria of lncRNAs identification. Similar to the characteristics reported previously (Li et al., 2017), cassava lncRNAs were evenly distributed across the chromosomes and the majority of them contained 2–3 exons, although the median length was much shorter in our case. To reveal the intersection and specificity of cassava lncRNAs in response to PEG and MT treatments, the transcriptional levels of lncRNAs affected by these two treatments were investigated, respectively. Totally 185 DE lncRNAs were identified, of which 75 (40%) are PEG-specific, 68 (37%) are MT-specific, and the remaining 42 (23%) are commonly responsive to both PEG and MT treatments (Fig. 3D). The proportions of DE lncRNAs, to a certain extent, might reflect the demand of lncRNA members executing different/common functions to deal with these two stresses.

Since numerous evidences have demonstrated that lncRNAs can act in *trans* to regulate the expression of multiple genes located throughout the genome (Huarte et al., 2010), a gene co-expression network of DE lncRNAs and protein-coding genes was performed in our study. According to the expression profiles, tens of lncRNAs, together with their co-expressed genes, were specifically high-expressed at each time-point across the stress treatments, exhibiting stress-specific expression patterns (Fig. 4A). These results indicated that lncRNAs responded to abiotic stress via a way of stress-specific expression regulation, which was directly or indirectly supported by the findings in previous studies (Di et al., 2014; Li et al., 2017; Zeng et al., 2017). Functional category enrichment revealed that PEG-uniquely-responsive lncRNAs mainly participated in RNA regulation of transcription, calcium signaling, mitochondrial electron transport/ATP synthesis, hormone metabolism, and transport. Consistently, in cotton, Lu et al. (2016) concluded that lncRNAs were likely to involve in regulating plant hormone pathways in response to drought stress; in *Arabidopsis*, lncRNA DRIR participated in the expression regulation of genes involved in ABA signaling and water transport under drought condition (Qin et al., 2017); in cassava, Li et al. (2017) found that transcriptional regulation of gene expression (especially the genes involved in hormone signal transduction and secondary metabolic pathways) might be one of the principal roles of lncRNAs in response to drought and/or cold stresses. On the contrary, currently no information was available regarding the functions of lncRNAs in response to MT treatment in plants. In our study, we revealed that MT-uniquely-responsive lncRNAs were mainly involved in tetrapyrrole synthesis, cytochrome P450, and cell wall modification, supporting that MT played major roles in photosystem protection, ROS-scavenge, cell wall, cell division, fatty acid biosynthesis, and secondary metabolism (Shi et al., 2015; Wei et al., 2015; Zhao et al., 2015). Moreover, our study also revealed that MT and PEG both-responsive lncRNAs were mainly involved in light reaction of photosynthesis, light signaling, FA synthesis and FA elongation, secondary metabolism, and tetrapyrrole synthesis. These results provide a general overview of the cross-talk or functional overlap of lncRNAs involved in the signaling regulation of MT and drought stress in plants.

In addition, lncRNAs can act *in cis* to regulate the expression of their neighboring genes. For example, in maize, the long non-coding RNA *Vgt1* influenced the expression of *ZmRap2* which located ~70 kb downstream of *Vgt1* (Li et al., 2014). In this study, a total of 28 lncRNA-mRNA pairs associated with *cis*-acting regulation were identified, and the expression of partial lncRNAs was verified by qRT-PCR (Table. S1). The adjacent genes influenced by these lncRNAs were involved in calcium signaling, RNA regulation of transcription, ABA and ethylene

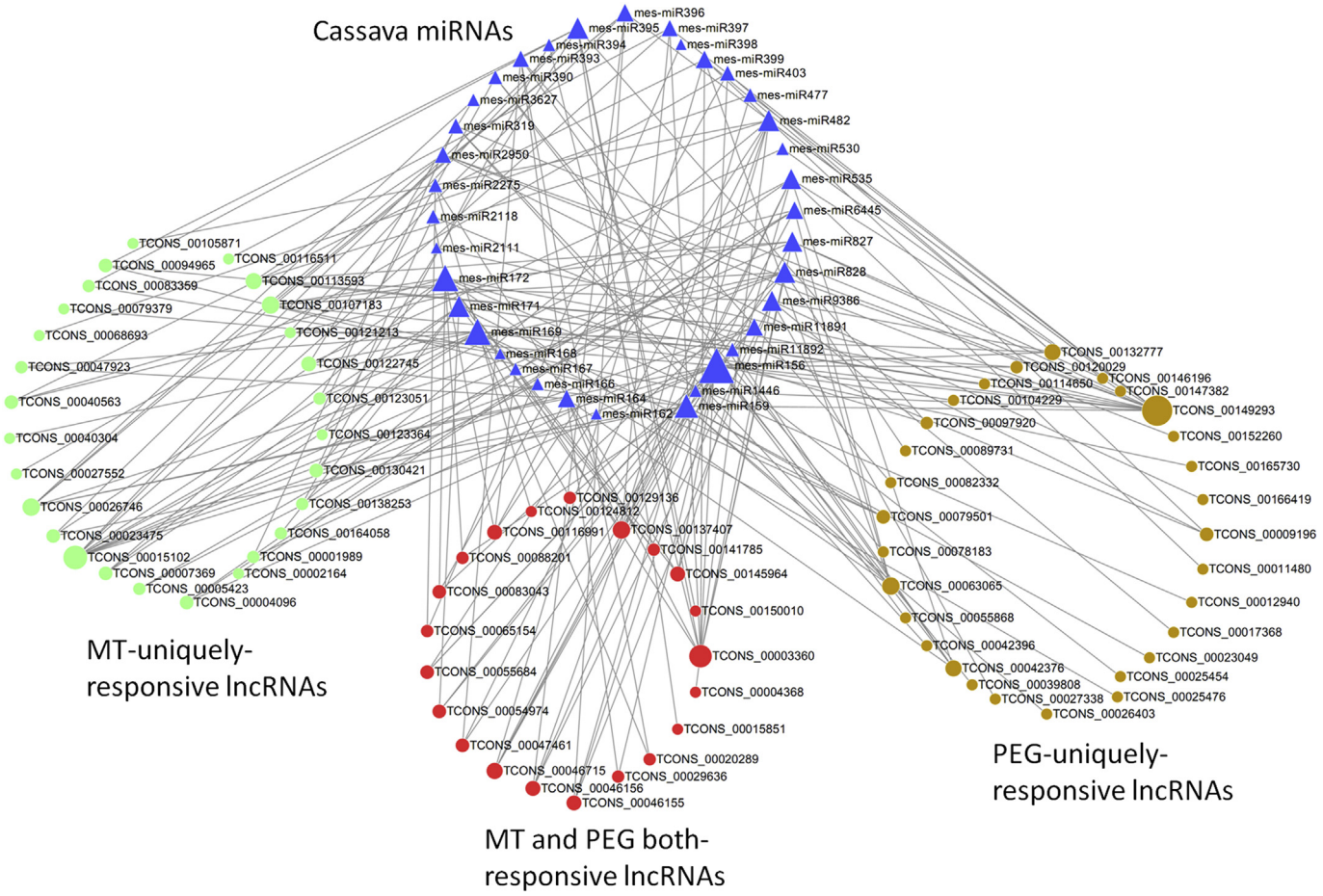

Fig. 5. A representative network of lncRNA-miRNA interaction. Cassava miRNAs were represented by blue triangles, while MT-uniquely-responsive lncRNAs, PEG-uniquely-responsive lncRNAs, and MT and PEG both-responsive lncRNAs were represented by light-green, gold, and red cycles, respectively. The node size was determined according to their degrees/connections to others. (For interpretation of the references to colour in this figure legend, the reader is referred to the Web version of this article.)

metabolisms, and redox homeostasis. These results, together with a previous report (Li et al., 2017), will provide a good foundation for further investigation of the molecular mechanisms and regulatory functions of lncRNAs in cassava.

Besides, lncRNAs can also be directly targeted by miRNAs for cleavage and degradation (Fan et al., 2015; Shuai et al., 2014). In recent years, computational methods were applied to identify lncRNAs functioned as putative miRNA targets in plants (Dai et al., 2018). In our study, 113 lncRNAs were predicted as potential targets of 153 miRNAs using bioinformatics. Specifically, three lncRNAs (TCONS_00149293, TCONS_00025454, and TCONS_00079501) were commonly targeted by several miRNAs including mes-miR156b/e, mes-miR159b, and mes-miR169v/ac, which were functional conserved and involved in ABA-mediated transcriptional regulation (Patanun et al., 2013). As expected, two genes of *HAI3* and *ABA2*, which participated in ABA signaling pathways, were found to be co-expressed with these lncRNAs. Besides, several genes involved in oxidative reaction (*CYP78A9*, *CYP82C2*, and *CYP714A1* encoding cytochrome P450), RNA regulation of transcription (*HSFC1*, *CRF2*, and *OZF1*), light signaling (*ELIP1*), transport (*TIL*), and major CHO metabolism (*SBE2*) were also co-expressed with these lncRNAs (Fig. 6 and Table. S4). Interestingly, genes involved in many of these pathways were induced by drought or melatonin treatment (Fu et al., 2016; Shi et al., 2015; Zeng et al., 2017). Together, these results indicated a complex regulation network of lncRNAs involved in MT and drought stresses in cassava. However, the regulatory mechanisms still need to be further studied.

5. Conclusion

In this study, a large number of lncRNAs responsive to PEG and/or MT treatment were identified, their distributions of chromosome location, transcript length, and exon number were investigated, and their potential functions were predicted via *trans*-acting, *cis*-acting, and miRNA targets. These findings provide a comprehensive view of cassava lncRNAs in response to abiotic stress, which will enable in-depth functional analysis in the near future. For examples, TCONS_00003360, TCONS_00015102, and TCONS_00149293 are the crucial candidates probably involved in ABA-participated gene regulation in abiotic stress of cassava via miRNA-lncRNA interaction, therefore their functions specifically deserve to be further characterized.

Authors' contributions

WH and GH conceived the idea and designed the experiments. ZD, CW, WT, and YY performed the experiments. ZD, CW, and WT analyzed the data. ZD and WT wrote the draft. ZD, WH, and GH finalized the manuscript.

Availability of data and material

The datasets generated and analyzed in the current study are submitted to the NCBI database under the accession of SRP156653.

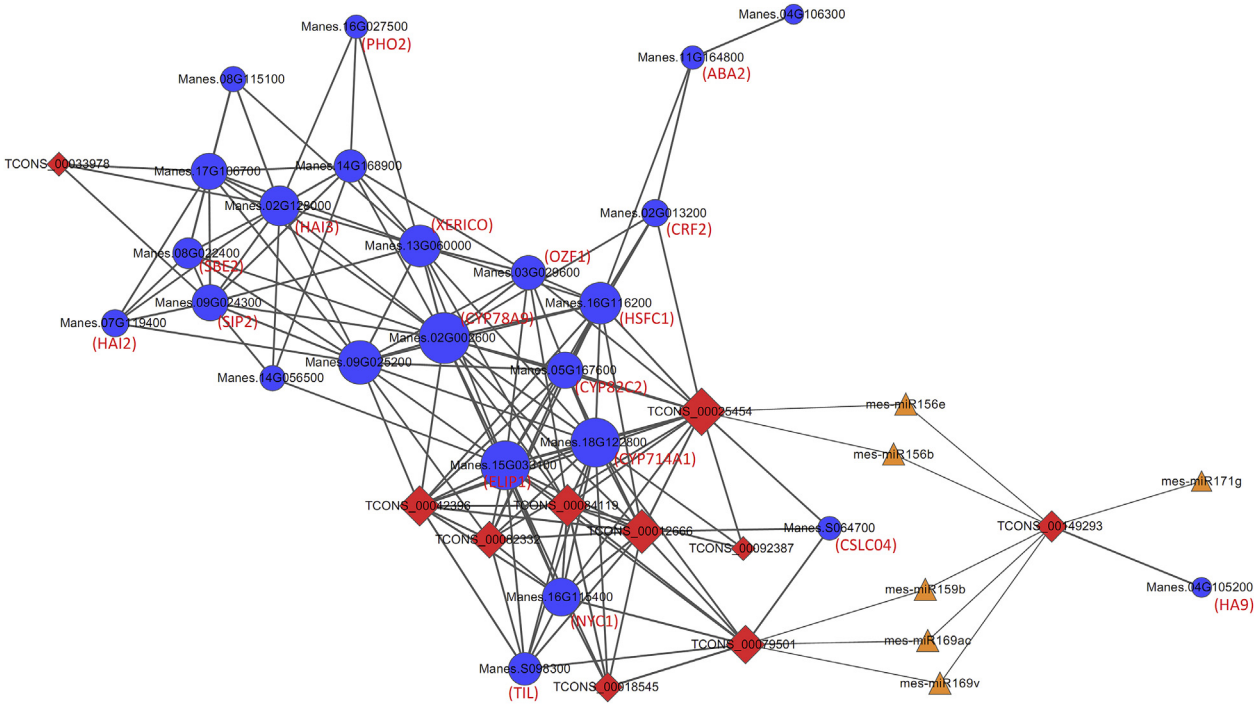

Fig. 6. A representative network of lncRNAs, miRNAs, and the genes involved in ABA signaling. Genes, lncRNAs, and miRNAs were represented by blue cycles, red diamonds, and yellow triangles, respectively, and their sizes were determined according to their degrees/connections to others. The gene names were in red in the brackets. (For interpretation of the references to colour in this figure legend, the reader is referred to the Web version of this article.)

Conflicts of interest

The authors declare no conflict of interest.

Acknowledgements

This work was supported by the Natural Science Foundation of Hainan Province (318MS092), the Central Public-Interest Scientific Institution Basal Research Fund for Chinese Academy of Tropical Agricultural Sciences (1630012019009, 1630052017021, 1630052016005, 1630052016006), the Central Public-Interest Scientific Institution Basal Research Fund for Innovative Research Team Program of CATAS (17CXTD-28, 1630052017017), and the earmarked fund for Modern Agro-industry Technology Research System (CARS-11). We also thank Dr. Wenquan Wang for the providing of cassava materials.

Appendix A. Supplementary data

Supplementary data to this article can be found online at https://doi.org/10.1016/j.plaphy.2019.05.008.

References

Antoniou, C., Chatzimichail, G., Xenofontos, R., Pavlou, J.J., Panagiotou, E., Christou, A., Fotopoulos, V., 2017. Melatonin systemically ameliorates drought stress-induced damage in Medicago sativa plants by modulating nitro-oxidative homeostasis and proline metabolism. J. Pineal Res. 62, e12401.

Arnao, M.B., Hernandez-Ruiz, J., 2018. Melatonin and its relationship to plant hormones. Ann. Bot. 121, 195–207.

Cai, B., Ma, W., Bi, C., Yang, F., Zhang, L., Han, Z., Huang, Q., Ding, F., Li, Y., Yan, G., Pan, Z., Yang, B., Lu, Y., 2016. Long noncoding RNA H19 mediates melatonin inhibition of premature senescence of c-kit(+) cardiac progenitor cells by promoting miR-675. J. Pineal Res. 61, 82–95.

Chekanova, J.A., 2015. Long non-coding RNAs and their functions in plants. Curr. Opin. Plant Biol. 27, 207–216.

Cui, G., Zhao, X., Liu, S., Sun, F., Zhang, C., Xi, Y., 2017. Beneficial effects of melatonin in overcoming drought stress in wheat seedlings. Plant Physiol. Biochem. 118, 138–149.

Dai, X., Zhuang, Z., Zhao, P.X., 2018. psRNATarget: a plant small RNA target analysis server (2017 release). Nucleic Acids Res. 46, W49–W54.

Di, C., Yuan, J., Wu, Y., Li, J., Lin, H., Hu, L., Zhang, T., Qi, Y., Gerstein, M.B., Guo, Y., Lu, Z.J., 2014. Characterization of stress-responsive lncRNAs in Arabidopsis thaliana by integrating expression, epigenetic and structural features. Plant J. 80, 848–861.

Eddy, S.R., 2009. A new generation of homology search tools based on probabilistic inference. Genome. Inform. 23, 205–211.

Fan, C., Hao, Z., Yan, J., Li, G., 2015. Genome-wide identification and functional analysis of lincRNAs acting as miRNA targets or decoys in maize. BMC Genomics 16, 793.

Ferdous, J., Hussain, S.S., Shi, B.J., 2015. Role of microRNAs in plant drought tolerance. Plant Biotechnol. J 13, 293–305.

Franco-Zorrilla, J.M., Valli, A., Todesco, M., Mateos, I., Puga, M.I., Rubio-Somoza, I., Leyva, A., Weigel, D., Garcia, J.A., Paz-Ares, J., 2007. Target mimicry provides a new mechanism for regulation of microRNA activity. Nat. Genet. 39, 1033–1037.

Fu, J., Wu, Y., Miao, Y., Xu, Y., Zhao, E., Wang, J., Sun, H., Liu, Q., Xue, Y., Xu, Y., 2017. Improved cold tolerance in Elymus nutans by exogenous application of melatonin may involve ABA-dependent and ABA-independent pathways. Sci. Rep. 7, 39865.

Fu, L., Ding, Z., Han, B., Hu, W., Li, Y., Zhang, J., 2016. Physiological investigation and transcriptome analysis of polyethylene glycol (PEG)-induced dehydration stress in cassava. Int. J. Mol. Sci. 17, 283.

Hu, W., Kong, H., Guo, Y., Zhang, Y., Ding, Z., Tie, W., Yan, Y., Huang, Q., Peng, M., Shi, H., Guo, A., 2016. Comparative physiological and transcriptomic analyses reveal the actions of melatonin in the delay of postharvest physiological deterioration of cassava. Front. Plant Sci. 7, 736.

Huarte, M., Guttman, M., Feldser, D., Garber, M., Koziol, M.J., Kenzelmann-Broz, D., Khalil, A.M., Zuk, O., Amit, I., Rabani, M., Attardi, L.D., Regev, A., Lander, E.S., Jacks, T., Rinn, J.L., 2010. A large intergenic noncoding RNA induced by p53 mediates global gene repression in the p53 response. Cell 142, 409–419.

Kong, L., Zhang, Y., Ye, Z.Q., Liu, X.Q., Zhao, S.Q., Wei, L., Gao, G., 2007. CPC: assess the protein-coding potential of transcripts using sequence features and support vector machine. Nucleic Acids Res. 35, W345–W349.

Langfelder, P., Horvath, S., 2008. WGCNA: an R package for weighted correlation network analysis. BMC Bioinf. 9, 559.

Li, C., Tan, D.X., Liang, D., Chang, C., Jia, D., Ma, F., 2015. Melatonin mediates the regulation of ABA metabolism, free-radical scavenging, and stomatal behaviour in two Malus species under drought stress. J. Exp. Bot. 66, 669–680.

Li, L., Eichten, S.R., Shimizu, R., Petsch, K., Yeh, C.T., Wu, W., Chettoor, A.M., Givan, S.A., Cole, R.A., Fowler, J.E., Evans, M.M., Scanlon, M.J., Yu, J., Schnable, P.S., Timmermans, M.C., Springer, N.M., Muehlbauer, G.J., 2014. Genome-wide discovery and characterization of maize long non-coding RNAs. Genome Biol. 15, R40.

Li, S., Yu, X., Lei, N., Cheng, Z., Zhao, P., He, Y., Wang, W., Peng, M., 2017. Genome-wide identification and functional prediction of cold and/or drought-responsive lncRNAs in cassava. Sci. Rep. 7, 45981.

Lu, X., Chen, X., Mu, M., Wang, J., Wang, X., Wang, D., Yin, Z., Fan, W., Wang, S., Guo, L., Ye, W., 2016. Genome-wide analysis of long noncoding RNAs and their responses to drought stress in cotton (Gossypium hirsutum L.). PLoS One 11, e0156723.

Okogbenin, E., Setter, T.L., Ferguson, M., Mutegi, R., Ceballos, H., Olasanmi, B., Fregene, M., 2013. Phenotypic approaches to drought in cassava: review. Front. Physiol. 4, 93.

Patanun, O., Lertpanyasampatha, M., Sojikul, P., Viboonjun, U., Narangajavana, J., 2013. Computational identification of microRNAs and their targets in cassava (Manihot esculenta Crantz.). Mol. Biotechnol. 53, 257–269.
Qin, T., Zhao, H., Cui, P., Albesher, N., Xiong, L., 2017. A nucleus-localized long non-coding RNA enhances drought and salt stress tolerance. Plant Physiol. 175, 1321–1336.
Shannon, P., Markiel, A., Ozier, O., Baliga, N.S., Wang, J.T., Ramage, D., Amin, N., Schwikowski, B., Ideker, T., 2003. Cytoscape: a software environment for integrated models of biomolecular interaction networks. Genome Res. 13, 2498–2504.
Shi, H., Chen, K., Wei, Y., He, C., 2016. Fundamental issues of melatonin-mediated stress signaling in plants. Front. Plant Sci. 7, 1124.
Shi, H., Jiang, C., Ye, T., Tan, D.X., Reiter, R.J., Zhang, H., Liu, R., Chan, Z., 2015. Comparative physiological, metabolomic, and transcriptomic analyses reveal mechanisms of improved abiotic stress resistance in bermudagrass [Cynodon dactylon (L). Pers.] by exogenous melatonin. J. Exp. Bot. 66, 681–694.
Shuai, P., Liang, D., Tang, S., Zhang, Z., Ye, C.Y., Su, Y., Xia, X., Yin, W., 2014. Genome-wide identification and functional prediction of novel and drought-responsive lincRNAs in Populus trichocarpa. J. Exp. Bot. 65, 4975–4983.
Sun, L., Luo, H., Bu, D., Zhao, G., Yu, K., Zhang, C., Liu, Y., Chen, R., Zhao, Y., 2013. Utilizing sequence intrinsic composition to classify protein-coding and long non-coding transcripts. Nucleic Acids Res. 41, e166.
Thimm, O., Blasing, O., Gibon, Y., Nagel, A., Meyer, S., Kruger, P., Selbig, J., Muller, L.A., Rhee, S.Y., Stitt, M., 2004. MAPMAN: a user-driven tool to display genomics data sets onto diagrams of metabolic pathways and other biological processes. Plant J. 37, 914–939.
Trapnell, C., Pachter, L., Salzberg, S.L., 2009. TopHat: discovering splice junctions with RNA-Seq. Bioinformatics 25, 1105–1111.
Trapnell, C., Roberts, A., Goff, L., Pertea, G., Kim, D., Kelley, D.R., Pimentel, H., Salzberg, S.L., Rinn, J.L., Pachter, L., 2012. Differential gene and transcript expression analysis of RNA-seq experiments with TopHat and Cufflinks. Nat. Protoc. 7, 562–578.
Utsumi, Y., Tanaka, M., Morosawa, T., Kurotani, A., Yoshida, T., Mochida, K., Matsui, A., Umemura, Y., Ishitani, M., Shinozaki, K., Sakurai, T., Seki, M., 2012. Transcriptome analysis using a high-density oligomicroarray under drought stress in various genotypes of cassava: an important tropical crop. DNA Res. 19, 335–345.
Wang, L., Park, H.J., Dasari, S., Wang, S., Kocher, J.P., Li, W., 2013a. CPAT: coding-Potential Assessment Tool using an alignment-free logistic regression model. Nucleic Acids Res. 41, e74.
Wang, P., Sun, X., Li, C., Wei, Z., Liang, D., Ma, F., 2013b. Long-term exogenous application of melatonin delays drought-induced leaf senescence in apple. J. Pineal Res. 54, 292–302.
Weeda, S., Zhang, N., Zhao, X., Ndip, G., Guo, Y., Buck, G.A., Fu, C., Ren, S., 2014. Arabidopsis transcriptome analysis reveals key roles of melatonin in plant defense systems. PLoS One 9, e93462.
Wei, W., Li, Q.T., Chu, Y.N., Reiter, R.J., Yu, X.M., Zhu, D.H., Zhang, W.K., Ma, B., Lin, Q., Zhang, J.S., Chen, S.Y., 2015. Melatonin enhances plant growth and abiotic stress tolerance in soybean plants. J. Exp. Bot. 66, 695–707.
Wu, H.J., Wang, Z.M., Wang, M., Wang, X.J., 2013. Widespread long noncoding RNAs as endogenous target mimics for microRNAs in plants. Plant Physiol. 161, 1875–1884.
Ye, N., Zhu, G., Liu, Y., Li, Y., Zhang, J., 2011. ABA controls H(2)O(2) accumulation through the induction of OsCATB in rice leaves under water stress. Plant Cell Physiol. 52, 689–698.
Yuan, J., Li, J., Yang, Y., Tan, C., Zhu, Y., Hu, L., Qi, Y., Lu, Z.J., 2018. Stress-responsive regulation of long non-coding RNA polyadenylation in Oryza sativa. Plant J. 93, 814–827.
Zeng, C., Ding, Z., Zhou, F., Zhou, Y., Yang, R., Yang, Z., Wang, W., Peng, M., 2017. The discrepant and similar responses of genome-wide transcriptional profiles between drought and cold stresses in cassava. Int. J. Mol. Sci. 18, 2668.
Zhang, N., Sun, Q., Zhang, H., Cao, Y., Weeda, S., Ren, S., Guo, Y.D., 2015. Roles of melatonin in abiotic stress resistance in plants. J. Exp. Bot. 66, 647–656.
Zhang, N., Zhao, B., Zhang, H.J., Weeda, S., Yang, C., Yang, Z.C., Ren, S., Guo, Y.D., 2013. Melatonin promotes water-stress tolerance, lateral root formation, and seed germination in cucumber (Cucumis sativus L.). J. Pineal Res. 54, 15–23.
Zhang, W., Han, Z., Guo, Q., Liu, Y., Zheng, Y., Wu, F., Jin, W., 2014. Identification of maize long non-coding RNAs responsive to drought stress. PLoS One 9, e98958.
Zhang, Y., Liu, X., Bai, X., Lin, Y., Li, Z., Fu, J., Li, M., Zhao, T., Yang, H., Xu, R., Li, J., Ju, J., Cai, B., Xu, C., Yang, B., 2018. Melatonin prevents endothelial cell pyroptosis via regulation of long noncoding RNA MEG3/miR-223/NLRP3 axis. J. Pineal Res. 64, e12449.
Zhao, H., Xu, L., Su, T., Jiang, Y., Hu, L., Ma, F., 2015. Melatonin regulates carbohydrate metabolism and defenses against Pseudomonas syringae pv. tomato DC3000 infection in Arabidopsis thaliana. J. Pineal Res. 59, 109–119.